(Preprint) AAS 17-032

CHARACTERIZATION OF GUIDANCE ALGORITHM PERFORMANCE FOR DRAG MODULATION-BASED AEROCAPTURE

Michael S. Werner* and Robert D. Braun†

Discrete-event drag modulation systems are an attractive option for flight control during aerocapture. These systems require precise timing of the drag modulation events to ensure accurate final orbit delivery. Two different guidance schemes for discrete-event drag-modulated aerocapture are evaluated: a heuristic deceleration profile curve-fit method and a higher-fidelity numeric predictor-corrector algorithm. The accuracy and computational performance of these algorithms is examined in a series of Monte-Carlo simulations of aerocapture missions at Earth, Mars, and Titan. Results indicate that while the deceleration curve-fit method requires minimal amounts of computation time, additional modifications must be made to ensure its robustness to day-of-flight uncertainties. At both low and medium guidance rates, the numeric predictor-corrector algorithm is able to effectively guide drag modulation events in the face of uncertainty.

INTRODUCTION

Aerocapture is an orbital maneuver in which a spacecraft utilizes atmospheric drag to capture directly into a target orbit. For missions to atmospheric worlds, aerocapture has long been considered a compelling technique that can offer significant reductions in fuel mass and total cost[1]. Numerous conceptual studies have advanced the technical maturity of aerocapture, to help enable its use on missions to different targets. Despite the conceptual readiness and potential benefits of aerocapture, use of the technique has been inhibited by its perceived risk, complexity, and lack of an in-flight demonstration[2, 3].

Simplifying the typical aerocapture flight system may help facilitate its use on future flight missions. One source of complexity is the control scheme required to target a specific final orbit. Historically, lift modulation has been the main suggestion for aerocapture control[4, 5]. Lift modulation control schemes involve modifying a vehicle's effective lift-to-drag ratio, either through changes in bank angle or angle-of-attack. These changes may require a spacecraft with asymmetric flight geometries and intricate effectors. For a potentially high-risk aerocapture maneuver, the complexities of lift modulation could be undesirable.

* Graduate Research Assistant, School of Aerospace Engineering, Georgia Institute of Technology, 270 Ferst Drive, Atlanta, GA, 30318.
† Dean, College of Engineering and Applied Science, University of Colorado Boulder, 1111 Engineering Drive, Boulder, CO, 80309.

Drag modulation flight control has recently been suggested as a means of greatly reducing the complexity of aerocapture systems. Drag modulation systems alter a vehicle's ballistic coefficient, β, in order to effect control over its trajectory:

$$\beta = \frac{m}{C_D A} \tag{1}$$

where m is the vehicle's mass, C_D is its hypersonic drag coefficient, and A is its aerodynamic reference area. When compared to lift modulation, drag modulation techniques enable the use of modest avionics algorithms, sensors, and actuators, and eliminate the need for center-of-gravity offset and an onboard propulsive reaction control system. As a result, drag modulation is a promising technique for facilitating simplistic aerocapture mission architectures.

The most basic form of drag modulation flight control for aerocapture is a single-stage jettison system, shown in Figure 1. At atmospheric interface, the vehicle is flying with a large drag skirt attached, increasing its drag area and thereby lowering its β to β_1. Within the atmosphere, once enough energy has been dissipated to achieve the target orbit, the drag skirt is jettisoned, increasing the spacecraft's β to β_2. As a result of this increase, the vehicle experiences greatly reduced deceleration through atmospheric egress.

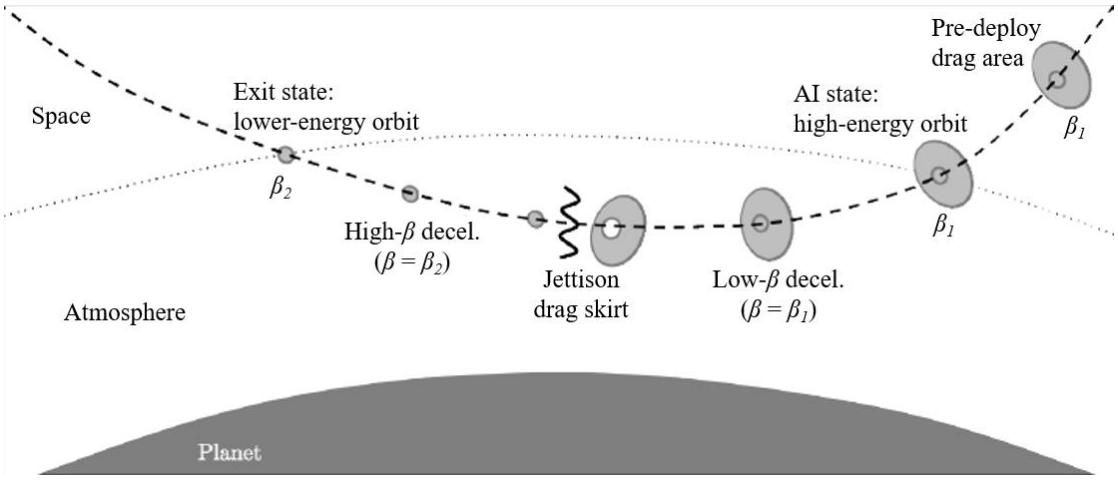

Figure 1. Single-Event Drag Modulation Diagram[6].

While these types of single-stage systems can help minimize mechanical complexity, their only source of control authority is the jettison event. Accurate timing of this event is therefore required to achieve the desired post-aerocapture orbit in the face of atmospheric and trajectory uncertainties. Appropriate guidance algorithm selection is necessary to help reduce errors in jettison timing.

Past investigations into discrete-event drag-modulated aerocapture exist, but research on realistic guidance performance is limited. Two studies by Putnam, Braun, and Clark make use of a numeric predictor-corrector (NPC) algorithm for guidance of drag-modulated aerocapture systems at Earth, Mars, Venus, and Titan[6, 7]. The accuracy exhibited by their NPC algorithm is promising, although Putnam et al. note its relative computational complexity. This algorithm was applied in recent work to facilitate a smallsat mission concept for an aerocapture flight demonstration at Earth[8]. The conservative guidance rate used in this investigation resulted in a decrease in final orbit accuracy when compared to the aforementioned studies. As such, for aerocapture missions with

limited computational resources available, a less-intensive guidance algorithm option may be desirable.

Johnson and Lyons present a guidance method in which accelerometer measurements are fit to a pre-generated deceleration curve, in order to target single-event-jettison trajectories for aerocapture at Titan[9]. Guidance algorithms of this fidelity may be well suited for simplistic aerocapture missions, as they require a minimal amount of calculation and instrumentation. However, the deceleration curve-fit (DCF) method developed by Johnson and Lyons is for a vehicle with a very large ratio of pre- and post-jettison ballistic coefficients (β_2/β_1), and is based on a monotonically-decreasing relationship between sensed deceleration at jettison and timing of the jettison event. An alternative approach is required for vehicles that may jettison before or after peak deceleration has been reached.

Early Mars landers are perhaps the most well-known historical examples of controlling discrete-event drag modulation events with limited computational abilities. In particular, Mars Pathfinder utilized an elegant curve-fit method to time its parachute deployment[10]. The algorithm used by Pathfinder requires just two distinct accelerometer measurements, and can readily be extended to time discrete drag modulation events for aerocapture.

The purpose of this study is to examine the performance of different potential guidance algorithms for drag-modulated aerocapture at Earth, Mars and Titan. The following guidance algorithm configurations are considered:

1. A Mars Pathfinder-inspired DCF guidance method
2. An NPC algorithm running at a low guidance rate
3. An NPC algorithm running at a medium guidance rate

The results of this investigation can help characterize the trade-off between guidance algorithm computational intensity and accuracy of the delivered final orbit for single-event-jettison aerocapture systems.

METHODOLOGY

Trajectory Modeling

A numeric trajectory simulation was used in this study to analyze the atmospheric portions of the aerocapture trajectories. The simulation integrates the planar equations of motion using a 4th-order Runge Kutta scheme with a constant 0.02 second time step. Planetary bodies were modeled as spheres, with inverse-square gravity and J2 perturbations. Nominal planetary atmospheres were formulated as a table look-up of different atmospheric properties as a function of altitude; these properties were generated via the Global Reference Atmospheric Model (GRAM) software for each planetary body[11]. Orbital properties at atmospheric exit were used by the trajectory simulation to determine the spacecraft's post-aerocapture orbit.

Guidance Methods

Numeric Predictor-Corrector. The NPC algorithm used for this study is described in detail in Reference 6. The predictor phase of the algorithm uses accelerometer measurements to numerically propagate the spacecraft's current trajectory, in order to determine its state at atmospheric exit. The corrector uses this state to calculate the vehicle's post-aerocapture orbit and then adjusts the timing of the drag skirt jettison event accordingly, with the goal of minimizing error in final apoapsis altitude. The NPC also features a constant-bias atmospheric density correction factor to improve accuracy in the face of atmospheric uncertainties.

Deceleration Curve-Fit. The original implementation of the DCF algorithm under consideration for this study can be seen in Reference 10, which describes the navigation processes used for Mars Pathfinder. As adapted to single-event-jettison aerocapture, the algorithm's structure is very similar. During atmospheric entry, the algorithm remains in standby until an initial deceleration value, g_1, is measured by the onboard accelerometers. After this measurement occurs, a timer is initiated. Once ΔT seconds have passed, a second deceleration measurement, g_2, is taken. This g_2 value is then compared against a pre-generated curve that maps g_2 measurements against time until jettison, t_{go}. The resulting t_{go} value is then used to schedule the jettison event.

As an example, the curve generated for Earth aerocapture in this study is shown in Figure 2, in the form of a best-fit 3rd degree polynomial that interpolates discrete g_2 and t_{go} pairings. The trajectories used to generate these pairings are configured such that jettison is guaranteed to occur at a time which minimizes errors in final apoapsis altitude. For this study, a simulated annealing optimization approach was used to obtain the ideal jettison times for 20 different curve-fit trajectories over a diverse range of entry flight path angles.

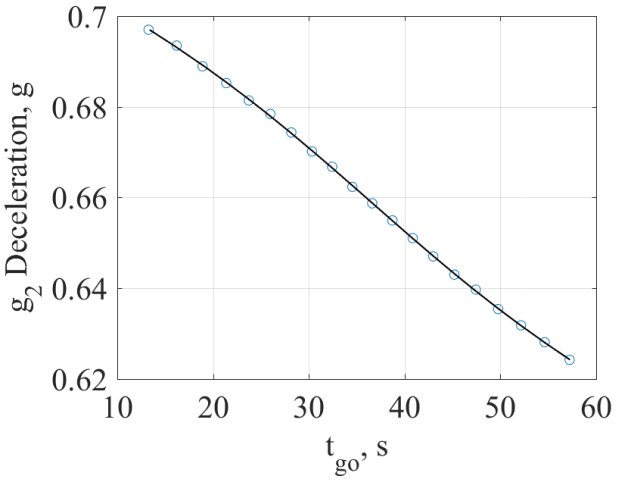

Figure 2. Jettison t_{go} Curve Fit for Earth Aerocapture.

Table 1. Deceleration Curve Fit Parameters.

Configuration	Parameter	Value
Single-event-jettison aerocapture	g_1	0.3 g's
	ΔT	10 s
Mars Pathfinder parachute timing	g_1	5 g's
	ΔT	12 s

Table 1 shows the configuration of the algorithm parameters used for aerocapture guidance in this study, alongside the configuration used by Mars Pathfinder. Although the low g_1 value specified can increase the likelihood of false or pre-emptive triggers in a real flight situation, it is necessary to account for the potential of inbound aerocapture trajectories with steeper-than-expected

entry flight-path angles, which require the jettison event to occur very early in atmospheric flight. The risks associated with this requirement can be mitigated by reducing uncertainty in entry state (enabling a higher g_1 value), or by taking a time-average of deceleration instead of an instantaneous measurement.

Spacecraft and Trajectory Design

Table 2 lists the key spacecraft design properties used for the single-event-jettison aerocapture missions in this study, while the nominal inbound trajectory parameters for these missions are shown in Table 3. A 60-degree sphere-cone form factor was used for the Earth vehicle and a 70-degree sphere-cone shape was assumed for the Mars and Titan spacecraft. It was assumed that the hypersonic drag coefficients of these vehicles are constant, and the trajectories were assumed to be ballistic. The entry velocity magnitudes and flight-path angles listed in Table 3 are inertial.

Table 2. Vehicle Design Parameters.

Planetary Body	Vehicle Configuration	Parameter	Value
Earth	Pre-jettison	Radius	0.25 m
		Mass	19.6 kg
		β	66.4 kg/m^2
	Post-jettison	Radius	0.10 m
		Mass	14.4 kg
		β	302.0 kg/m^2
Mars	Pre-jettison	Radius	1.00 m
		Mass	30.0 kg
		β	5.9 kg/m^2
	Post-jettison	Radius	0.30 m
		Mass	20.0 kg
		β	43.9 kg/m^2
Titan	Pre-jettison	Radius	5.00 m
		Mass	2000.0 kg
		β	15.8 kg/m^2
	Post-jettison	Radius	1.50 m
		Mass	1800.0 kg
		β	158.2 kg/m^2

A smallsat with a highly elliptical starting orbit was used as the baseline design for the Earth mission. The specific spacecraft design and mission concept used at Earth are identical to the flight test design described in Reference 8. As such, the results of this analysis can be used to help facilitate guidance algorithm selection for future development of this conceptual flight test mission.

At Mars, a smallsat-scale spacecraft design was used. This design is similar to the one used at Earth, but features a larger β_2/β_1 ratio in order to yield a wider entry flight-path angle corridor. The nominal trajectory flown by this spacecraft is eastbound equatorial, with the goal of capturing into

a low elliptical orbit. The entry flight-path angle selected was at the center of this vehicle's entry corridor for the desired target orbit.

Values from the literature were used as a baseline for the Titan mission. The inner radius was sized to the minimum packaging requirement listed for the Titan Explorer mission concept[5], and the spacecraft mass was also taken from this study. To achieve the desired 5-meter pre-jettison radius, the vehicle would likely utilize a deployable or inflatable drag device. For this study, it was assumed that the spacecraft is flying an eastbound equatorial trajectory and targeting a 4000-km post-aerocapture apoapsis altitude, to help minimize the chances of atmospheric re-entry following the maneuver. The entry flight-path angle was selected to center the desired orbit within the vehicle's targeting capability.

Table 3. Inbound Trajectory Properties.

Planetary Body	Parameter	Value
Earth	Entry velocity magnitude	10.3 km/s
	Entry flight-path angle	-5.04°
	Altitude at atmospheric interface	125 km
	Target orbit apoapsis altitude	1760 km
Mars	Entry velocity magnitude	6.0 km/s
	Entry flight-path angle	-11.08°
	Altitude at atmospheric interface	150 km
	Target orbit apoapsis altitude	1760 km
Titan	Entry velocity magnitude	6.5 km/s
	Entry flight-path angle	-46.33°
	Altitude at atmospheric interface	1700 km
	Target orbit apoapsis altitude	4000 km

Uncertainty Analysis

Monte Carlo simulations were run to examine the response of each guidance option to uncertainty. The specific dispersions applied for each mission are listed in Table 4. For the Earth simulation, the entry flight-path angle dispersion was obtained from Reference 8. Entry state uncertainties at Mars are based on MSL approach navigation results[12], and uncertainties at Titan were obtained from the Titan Explorer study[13]. Atmospheric density and wind variations were generated by the GRAM atmospheric models for each planetary body.

For the purposes of this study, the propulsive periapsis-raising maneuver that occurs following the atmospheric portion of aerocapture was not modeled. In real mission situations, this maneuver will add additional variation to the final orbit obtained, but the effect of these uncertainties are minor when compared to those introduced by the atmospheric portion.

Table 4. Monte Carlo Simulation Uncertainty Sources.

Planetary Body	Parameter	Dispersion
Earth	Entry flight-path angle	0.12°
	Hypersonic C_A	3%
	Hypersonic C_N	5%
	Atmospheric density & wind variations	Earth-GRAM
Mars	Entry flight-path angle	0.2°
	Entry velocity magnitude	2 m/s
	Hypersonic C_A	3%
	Hypersonic C_N	5%
	Atmospheric density & wind variations	Mars-GRAM
Titan	Entry flight-path angle	0.24°
	Entry velocity magnitude	5 m/s
	Hypersonic C_A	3%
	Hypersonic C_N	5%
	Atmospheric density & wind variations	Titan-GRAM

RESULTS

Curve-Fit Algorithm Validation

In order to validate the applicability of the Pathfinder DCF guidance algorithm to single-event-jettison aerocapture, a series of trajectories were run over a range of entry flight-path angles, with every other trajectory parameter held to the nominal values listed in Table 3. The guidance algorithm was called at the data acquisition rate for each mission: 50 Hz for Earth and Mars, and 25 Hz for Titan. Results for this validation analysis are shown in Figures 3, 4, and 5 for Earth, Mars, and Titan respectively.

These validation cases show that the curve-fit algorithm exhibits the ability to target the desired post-aerocapture apoapsis to an adequate degree of accuracy at Earth and Mars. The variations shown are indications of the extreme sensitivity of single-event-jettison systems to jettison timing. As an example, the trajectory with the greatest apoapsis altitude error in Figure 3 was examined. The ideal jettison time for this trajectory occurs 86.30 seconds after atmospheric entry and results in an apoapsis altitude of 1759.9 km. The curve-fit guidance algorithm determined that jettison should occur 320 milliseconds earlier, which led to a deviation of 66.7 km from the target.

Validation results at Titan display the greatest inaccuracies, with variations as large as 3500 km from the desired final apoapsis altitude. Even with these inaccuracies, all of the test cases were able to capture into orbit. A potential explanation for these variations is that, as designed, the Titan mission features the longest atmospheric flight times and the largest entry flight-path-angle corridor. These two factors lead to a larger distribution of potential jettison times than either of the other

two missions. Increasing the number of trajectories used to generate the initial deceleration curve-fit may improve the algorithm's performance by sampling this jettison time distribution more thoroughly.

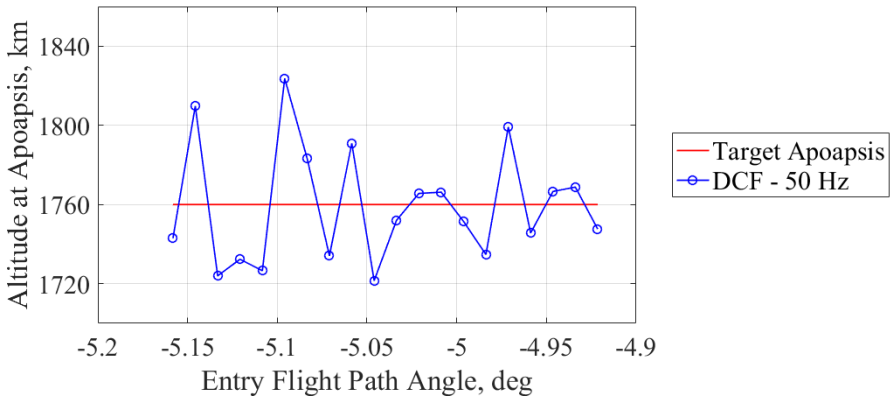

Figure 3. Earth DCF Algorithm Validation.

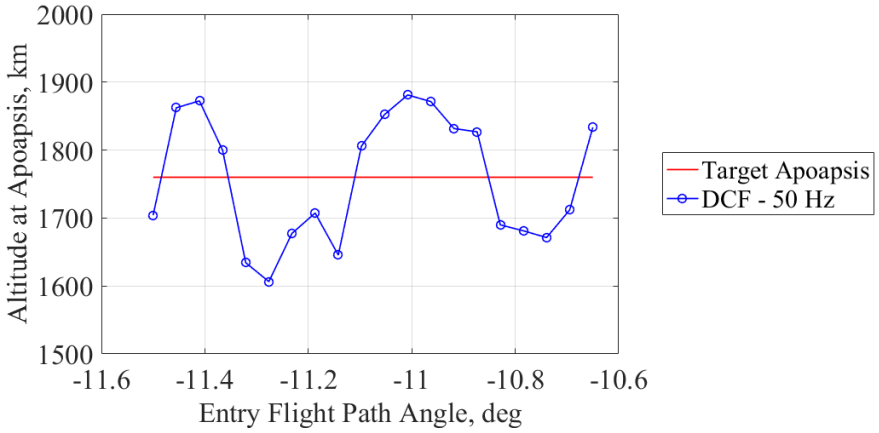

Figure 4. Mars DCF Algorithm Validation.

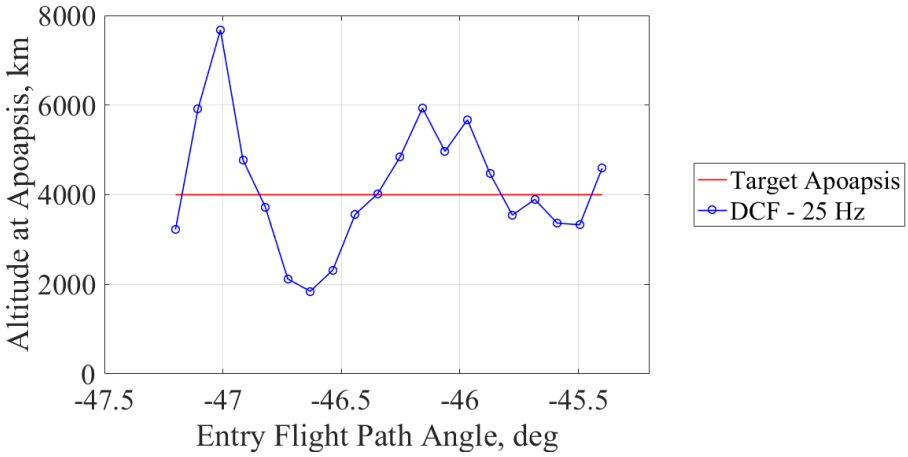

Figure 5. Titan DCF Algorithm Validation.

Monte Carlo Analysis

Results from the Monte Carlo analyses are listed in Table 5. 5000 samples were run for each combination of planetary body and guidance algorithm, with each sample targeting the final apoapsis altitudes given in Table 3. The statistics for post-maneuver apoapsis altitude were determined only from the successful cases – cases that involve surface impact or failure to capture into orbit were excluded.

The DCF guidance algorithm was the least computationally intensive option, despite the high guidance rates chosen at each planet. These rates match the spacecraft data acquisition rates to ensure accurate instantaneous deceleration measurements are achieved. Despite this, the curve-fit method performs quite poorly at all 3 planets, with a number of cases that either fail to escape the atmosphere or fail to capture into orbit. Even amongst the successful cases, there is a large degree of variation from the target.

During data post-processing, it was determined that atmospheric density variations were by far the leading cause of failure for the DCF method. Although the algorithm is somewhat robust to uncertainties in entry state and spacecraft aerodynamics, changes in atmospheric density profile lead to correlations between g_2 and t_{go} that are different than those expected for a nominal atmosphere. This trend can be seen by comparing the results for each planet: the failure rates are greater at Mars and especially Titan, where atmospheric uncertainties are much larger than at Earth. Atmospheric variations were less of a concern for the original implementation of this algorithm on Mars Pathfinder, because the mission was less sensitive to its parachute deployment time; excess velocity accrued could later be zeroed out (to an extent) by the propulsive maneuver that was performed prior to landing. For the purposes of single-event-jettison aerocapture missions, some means of accounting for these atmospheric uncertainties is most likely required for this DCF method to be a viable guidance choice.

At both low and medium guidance rates, the NPC algorithm was more effective at targeting the desired final orbit. The low-rate algorithm resulted in only 8 failures, all at Titan, while all of the mid-rate cases were successful at capturing into orbit. Both the low and mid-rate choices resulted in mean apoapsis altitudes that were slightly below target, which indicates that the algorithm has a tendency to predict later-than-optimal jettison times. Histograms of the NPC results, displayed in Figures 6 – 8, show that this tendency is more pronounced for the low-rate selection, which exhibits a slightly bimodal distribution at Earth and Mars as a result of these late jettisons. This shape is not present in results for the mid-rate group, which produces more accurate final orbits with less variation (albeit at the cost of increased computation time). At Titan, both the low- and mid-rate algorithms show a larger range of apoapsis altitudes, with mean values that are more than 500 km below the target. This is due in part to the additional atmospheric uncertainty at Titan, including strong winds that are present in the Titan-GRAM atmospheric model but not considered by the NPC's onboard model.

Table 5. 5000-Sample Monte Carlo Simulation Results.

Planetary Body	Parameter	Value		
Earth	Guidance scheme	DCF	Low-rate NPC	Mid-rate NPC
	Guidance execution rate	50 Hz	1 Hz	5 Hz
	Mean computation time	0.20 s	0.30 s	0.60 s
	Number of surface impacts	1729	0	0
	Number of escape trajectories	0	0	0
	Mean apoapsis altitude	4441.8 km	1677.2 km	1707.2 km
	3σ apoapsis altitude deviation	2532.2 km	60.7 km	31.3 km
	Apoapsis altitude range	11656.9 km	349.5 km	268.2 km
Mars	Guidance scheme	DCF	Low-rate NPC	Mid-rate NPC
	Guidance execution rate	50 Hz	1 Hz	5 Hz
	Mean computation time	0.32 s	0.53 s	1.25 s
	Number of surface impacts	1962	0	0
	Number of escape trajectories	1752	0	0
	Mean apoapsis altitude	4621.4 km	1732.2 km	1755.4 km
	3σ apoapsis altitude deviation	3239.9 km	65.72 km	22.1 km
	Apoapsis altitude range	11845.3 km	340.3 km	217.9 km
Titan	Guidance scheme	DCF	Low-rate NPC	Mid-rate NPC
	Guidance execution rate	25 Hz	0.5 Hz	2.5 Hz
	Mean computation time	1.21 s	1.31 s	2.46 s
	Number of surface impacts	2191	8	0
	Number of escape trajectories	2597	0	0
	Mean apoapsis altitude	4385.6 km	3093.4 km	3318.8 km
	3σ apoapsis altitude deviation	2938.4 km	485.4 km	504.2 km
	Apoapsis altitude range	11537.7 km	3116.9 km	3826.4 km

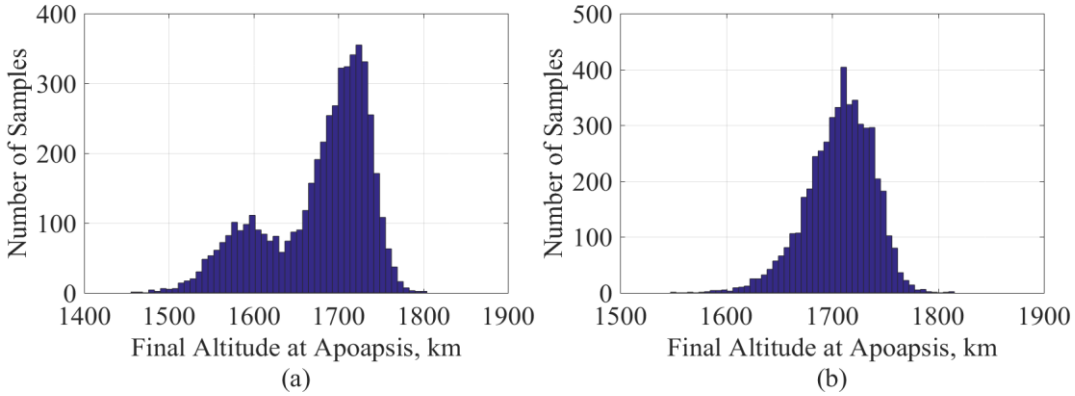

Figure 6. Earth Monte Carlo Histograms: (a) 1 Hz NPC, and (b) 5 Hz NPC.

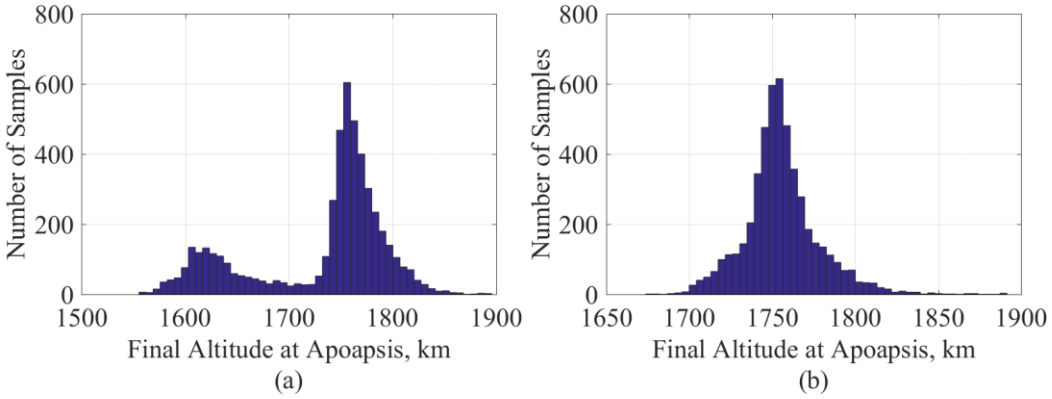

Figure 7. Mars Monte Carlo Histograms: (a) 1 Hz NPC, and (b) 5 Hz NPC.

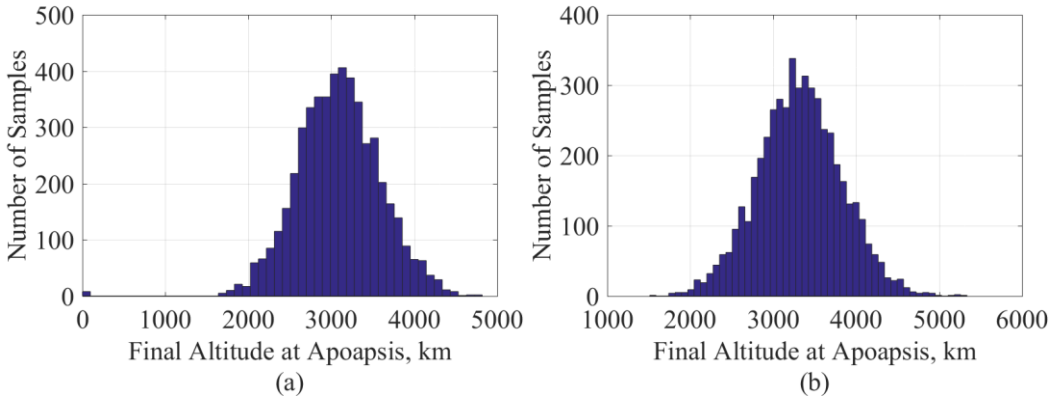

Figure 8. Titan Monte Carlo Histograms: (a) 0.5 Hz NPC, and (b) 2.5 Hz NPC.

CONCLUSIONS

For a nominal set of single-event-jettison aerocapture missions to Earth, Mars, and Titan, it was found that a Mars Pathfinder-based deceleration curve-fit approach to jettison guidance requires the least amount of computation time to arrive at a solution, even when called at a very high rate. Although this method performed adequately for nominal planetary atmospheres, it requires further modification to be able to account for day-of-flight atmospheric uncertainties.

The numeric predictor-corrector guidance algorithm was able to successfully target a desired post-aerocapture orbit in the face of uncertainties at both low and medium guidance execution rates. The computational time savings offered by the low-rate algorithm may be desirable for aerocapture missions in which precise final orbit targeting is not a requirement. For missions with greater accuracy requirements, it may be necessary to call this guidance algorithm at a higher rate, or consider different drag modulation control schemes (such as a multi-stage jettison approach.)

Future work for guidance of single-event-jettison systems could include the investigation of modifications to the deceleration curve-fit guidance approach, such as the consideration of different measurement and trigger options and the addition of an atmospheric density correction function to

help account for day-of-flight uncertainties. Should these modifications yield accuracy improvements, the curve-fit scheme may be worth revisiting as a computationally inexpensive guidance option. It may also be beneficial to consider other guidance control schemes, including other real-time predictive algorithms and potential analytic methods developed from the equations of motion.

CONCLUSIONS

The authors are grateful for the guidance of Dr. Zachary Putnam, of the University of Illinois at Urbana-Champaign.

This work was supported by a NASA Space Technology Research Fellowship.

REFERENCES

[1]Hall, J. L., Noca, M. A., and Bailey, R. W., "Cost-Benefit Analysis of the Aerocapture Mission Set," *Journal of Spacecraft and Rockets*, Vol. 42, No. 2, 2005, pp. 309-320.

[2]Hall, J. L., "An Overview of the ST-7 Aerocapture Flight Test Experiment," *AIAA Atmospheric Flight Mechanics Conference and Exhibit*, Monterey, CA, August 2002.

[3]Percy, T. K., Bright, E., and Torres, A. O., "Assessing the Relative Risk of Aerocapture Using Probabilistic Risk Assessment," *41st AIAA/ASME/SAE/ASEE Joint Propulsion Conference & Exhibit*, Tucson, AZ, July 2005.

[4]Masciarelli, J., Westhelle, C.H., Graves, C.A., "Aerocapture Guidance Performance for the Neptune Orbiter," *AIAA Atmospheric Flight Mechanics Conference and Exhibit*, Providence, RI, August 2004.

[5]Lockwood, M. K., "Titan Aerocapture Systems Analysis," *39th AIAA/ASME/SAE/ASEE Joint Propulsion Conference and Exhibit*, Huntsville, AL, July 2003.

[6]Putnam, Z. R., and Braun, R. D., "Drag Modulation Flight Control System Options for Planetary Aerocapture," *Journal of Spacecraft and Rockets*, Vol. 51, No. 1, 2014, pp. 139-150.

[7]Putnam, Z. R., Clark, I. G., and Braun, R. D., "Drag Modulation Flight Control for Aerocapture," *Aerospace Conference, 2012 IEEE*, Big Sky, MT, March 2012, pp. 1-10.

[8]Werner, M. S., et al., "Development of an Earth Smallsat Flight Test to Demonstrate Viability of Mars Aerocapture," *55th AIAA Aerospace Sciences Meeting*, Grapevine, TX, January 2017.

[9]Johnson, W. R. and Lyons, D. T., "Titan Ballute Aerocapture Using a Perturbed TitanGRAM Model," *AIAA Atmospheric Flight Mechanics Conference and Exhibit*, Providence, RI, August 2004.

[10]Braun, R. D., Spencer, D. A., Kallemeyn, P. H., and Vaughan, R. M, "Mars Pathfinder Atmospheric Entry Navigation Operations", *22nd Atmospheric Flight Mechanics Conference*, New Orleans, LA, August 1997.

[11]Duvall, A. L., Justus, C. G., and Keller, V. W., "Global Reference Atmospheric Model (GRAM) Series for Aeroassist Applications," *43rd AIAA Aerospace Sciences Meeting and Exhibit*, Reno, NV, Jan. 2005.

[12]Martin-Mur, T. J., Kruizinga, G. L., and Wong, M. C., "Mars Science Laboratory Interplanetary Navigation Analysis," *22nd International Symposium on Space Flight Dynamics*, São José dos Campos, Brazil, March 2011.

[13]Hanak, C. and Bishop, R. H., "Aerocapture at Titan and Neptune: Navigation Sensitivity Study," *9th AIAA Atmospheric Flight Mechanics Conference*, Providence, RI, Aug. 2004.